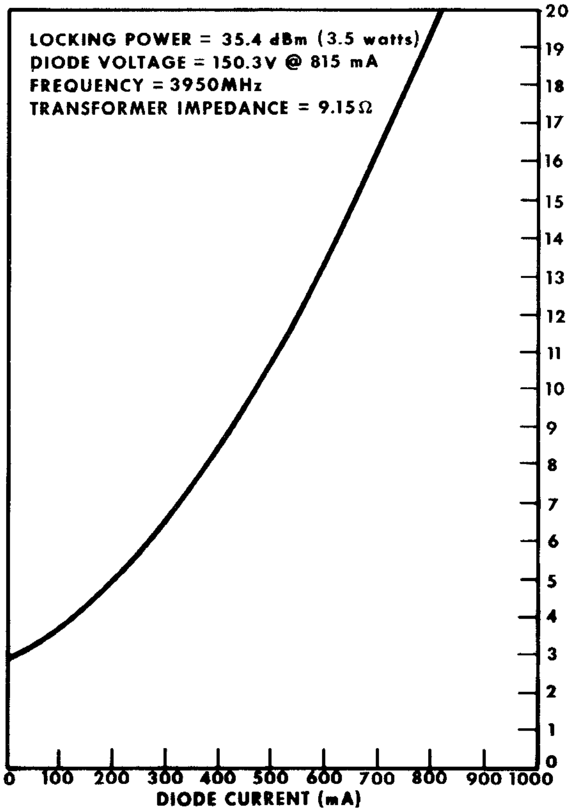

Fig. 6. Diode-triplet power output versus current. A 4-GHz amplifier.

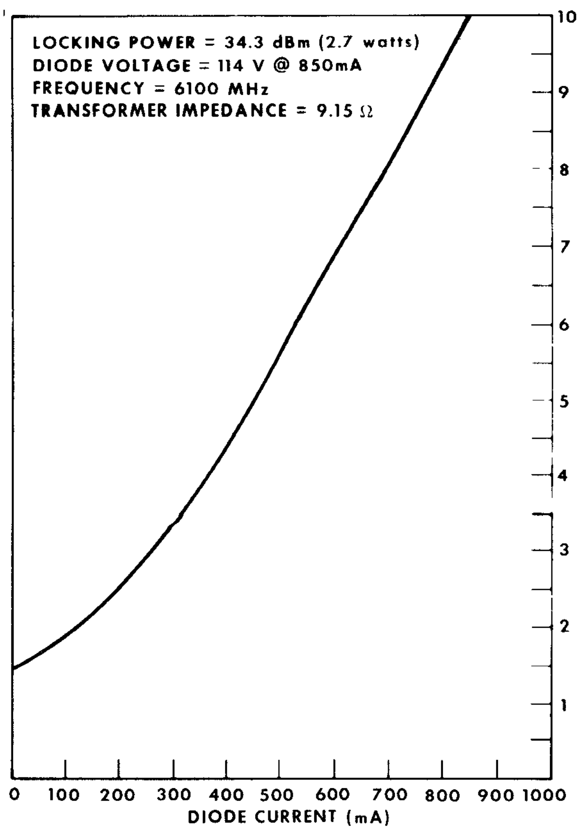

Fig. 7. Diode-triplet power output versus current. 6-GHz amplifier.

significant cost advantages: 1) use of a single tuned cavity with a single transformer, single dc supply circuit, and single set of harmonic filters for two or more IMPATT diodes, and 2) requirement of a single current-regulated source in place of two or more individually controlled current sources. Since the experiments were done with a very well matched pair and triplets of diodes, further studies concerning the necessary characteristics of the individual diodes to be grouped are required. Minor imbalances can be accepted if the amplifier performance is derated correspondingly. It has been shown to be feasible to extend this combining scheme to three or more diodes at both 4 and 6 GHz.

A possible disadvantage would be the unequal division of current for nonideally matched diodes which could necessitate some derating of the maximum dc power to assure acceptable reliability.

ACKNOWLEDGMENT

The authors wish to thank Dr. C. B. Swan for many helpful suggestions, especially for calling their attention to the "balancing resistor" scheme. Dr. J. C. Irvin's efforts to supply us with ever-better diodes are greatly appreciated.

REFERENCES

[1] I. Tatsuguchi, "A frequency-modulated phaselocked IMPATT power combiner," in *Digest 1970 Int. Solid-State Circuits Conf.* (Philadelphia, Pa., Feb. 1970), p. 18.
[2] J. W. Gewartowski, "Power combination with diode and circuit arrays," in *1970 IEEE Int. Conv. Digest*, Mar. 23–26, 1970, pp. 242–243.
[3] F. M. Magalhaes and W. O. Schlosser, "A microwave oscillator using series-connected IMPATT diodes," in *Proc. 1968 Int. Solid-State Circuits Conf.* (Philadelphia, Pa.), p. 150.
[4] C. B. Swan, private communication.
[5] C. T. Rucker, "A multiple-diode high-average-power avalanche-diode oscillator," *IEEE Trans. Microwave Theory Tech.* (Corresp.), vol. MTT-17, pp. 1156–1158, Dec. 1969.
[6] M. E. Hines, "Large-signal noise, frequency conversion, and parametric instabilities in IMPATT diode networks," *Proc. IEEE*, vol. 60, pp. 1534–1548, Dec. 1972.
[7] I. Tatsuguchi, N. R. Dietrich, and C. B. Swan, "Power-noise characterization of phase-locked IMPATT oscillators," *IEEE J. Solid-State Circuits* (*Special Issue on Solid-State Microwave Circuits*), vol. SC-7, pp. 2–10, Feb. 1972.

A New Method for Measuring Properties of Dielectric Materials Using a Microstrip Cavity

TATSUO ITOH, MEMBER, IEEE

***Abstract*—A new nondestructive method has been developed for measuring the dielectric constant and the loss factor of a slab-type material using a microstrip cavity. The method, which uses a simple and rapid substitution procedure, yields accurate results and has a number of advantages over currently available techniques. Experimental details and the theoretical basis are explained and experimental data are presented.**

I. INTRODUCTION

A number of methods are currently available for measuring the dielectric constant ϵ_r and the loss factor tan δ of a material at microwave frequencies. One typical example is the method based on the measurement of the electromagnetic scattering from the dielectric sphere placed in free space [1],[2]. Another common technique is the use of waveguides or waveguide cavities, which are either partially or completely filled with the dielectric materials to be measured. The ridge waveguide method [3] falls into this category.

Manuscript received October 19, 1973; revised December 19, 1973. This work was supported in part by the National Science Foundation under Grant GK 36854 and in part by the Army Research Office under Grant DA-ARO-D-31-124-G77.
The author is with the Department of Electrical Engineering, University of Illinois, Urbana, Ill. 61801.

In the strip-line method [4], developed recently, the unknown material is used as the dielectric filling medium in the triplate-type strip lines.

In designing microwave integrated circuits, accurate values of the dielectric constant and the loss factor of the substrate material must be known. A typical method for measuring the dielectric properties of substrate materials is the one reported by Napoli and Hughes [5]. In their method, both sides of the substrate plate are first metallized to form a parallel-plate resonator; the measurement of the resonant characteristics of such a reonator leads to the desired quantity. Similar methods were reported by Howell [6] and Ladbrooke *et al.* [7].

In this short paper, a new nondestructive method will be reported for measuring the dielectric properties of slab-type materials. The experimental procedure consists of a simple and rapid substitution technique which measures the resonant frequency and the Q factor of a microstrip cavity that is loaded with a slab of the dielectric to be measured. The inversion process used to derive the dielectric properties of the material from the measured data is readily performed with a computer.

The method has several advantages over other available methods. First, this method is nondestructive. Unlike the waveguide or waveguide cavity method, the unknown material does not have to be prepared in a specified size and/or shape. Second, the present method requires no reflection-free environment which is the basic requirement of the sphere methods [1],[2]. Third, in the method described in [4], only the effective dielectric constant is measured. On the other hand, the actual dielectric constant can be obtained in the method presented in this paper.[1] Furthermore, the present method is best suited to plastic materials, which are not amenable to measurement by the methods of [5], and, hence, it complements these other methods.[1]

In the next section, a brief theoretical explanation will be given for the present method of measurement. Experimental setups will be explained in Section III. The measurement and the computation procedures for deriving the dielectric properties will also appear in Section III. Finally, some experimental data will be presented in Section IV.

II. THEORY AND MEASUREMENT PROCEDURE

Fig. 1 shows the cross section of a microstrip line covered with a layer of dielectric material. Although the exact analysis shows that the modal field in the microstrip line is a hybrid one, a TEM approximation holds extremely well if the wavelength is chosen to be much larger than the width of the strip and the thickness of the substrate [8].

For a low-loss TEM transmission line, the attenuation and the phase constants are given by [9]

$$\alpha = \tfrac{1}{2}(LC)^{1/2}\left(\frac{R}{L} + \frac{G}{C}\right) \tag{1a}$$

$$\beta = \omega(LC)^{1/2} \tag{1b}$$

where R, G, L, and C are the resistance, conductance, inductance, and capacitance per unit length, respectively, and ω is the angular frequency.

Now consider two situations. 1) The overlay material is the reference material [Fig. 1(a)]. The reference material may be conveniently chosen to be the same as the substrate. 2) The reference material is replaced by the unknown dielectric material [Fig. 1(b)]. If the medium is nonmagnetic, the line inductance L remains unchanged regardless of the filling materials. Also, if the line resistance R is caused by the small loss in the conductors, the change in R is considered to be negligible for situations 1) and 2). Then

$$\frac{\beta_1\omega_2}{\beta_2\omega_1} = \left(\frac{C_1}{C_2}\right)^{1/2} \tag{2a}$$

$$\frac{2\alpha_1}{\beta_1}\omega_1 - \frac{2\alpha_2}{\beta_2}\omega_2 = \frac{G_1}{C_1} - \frac{G_2}{C_2} \tag{2b}$$

[1] The author expresses his sincere appreciation to the reviewer, who pointed out these advantages.

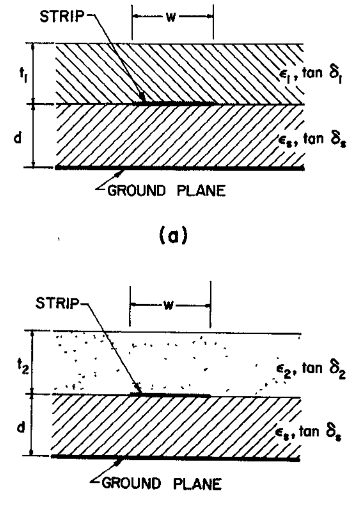

Fig. 1. (a) Cross section of microstrip line structure loaded with reference material. (b) Loaded with unknown material.

where the subscripts 1 and 2 designate the quantities for the situations 1) and 2), respectively.

Since the dielectric properties and the structural parameters are known for situation 1), the values of C_1 and G_1 can be found from (6) and (7) in the Appendix. Note that G_1 is associated with the dielectric loss in the filling materials. Hence, if we can obtain the values of the left-hand sides of (2a) and (2b) from some measurement, the values of C_2 and G_2 can be derived from (2a) and (2b).

It should now be noticed that C_2 and G_2 are, in turn, implicit functions of dielectric constant ϵ_2 and dissipation factor tan δ_2 ($= \sigma_2/\omega_2\epsilon_2$), i.e.,

$$C_2 = u(\epsilon_2) \tag{3a}$$

$$G_2 = v(\epsilon_2, \tan\delta_2) \tag{3b}$$

where the specific forms of u and v are given by (6) and (7). Since (3a) and (3b) are nonlinear, they cannot be solved analytically for ϵ_2 and tan δ_2. However, these values can be obtained numerically with desired accuracy using a root-seeking routine when the values of C_2 and G_2 are obtained from the measurement procedure.

Let us now turn to the measurement procedure to determine the left-hand sides of (2a) and (2b). To this end, a cavity consisting of a microstrip line can be used. As shown in Fig. 2, the cavity we have employed is essentially an open-ended microstrip line. The cavity will be loaded with the reference material and the unknown materials which correspond to situations 1) and 2), respectively. The open-ended microstrip line is believed to behave as an open-circuited line at low frequencies if it is hypothetically extended by Δl in order to account for the end effect. A value for Δl is usually $0.2d \sim 0.4d$ for the unloaded microstrip line with substrate of thickness d [10]. When the microstrip cavity is loaded with some material, the contribution of the loading to Δl at both ends is much smaller than that of the substrate. For this reason in the following computations Δl was assumed to be the same regardless of the loading materials. This assumption can, of course, be a source of error. However, since $d \ll l$ for long cavities used in this paper for UHF to low microwave frequencies, this error may well be negligible.

Let us now consider the case where the cavity is fed at frequencies ω_1 and ω_2 for the situations 1) and 2), respectively, so that the nth resonance is excited, i.e., the guide wavelength $\lambda = 2\bar{l}/n$, $n = 1,2,\cdots$, for both 1) and 2) situations where $\bar{l} = l + 2\Delta l$. Hence, the phase constants β_1 and β_2 are identical because $\beta = 2\pi/\lambda$. It is also well known that the Q factor of the open-circuited transmission line is given by

$$Q = \frac{\beta}{2\alpha}. \tag{4}$$

From the above argument, (2a) and (2b) can be expressed in a

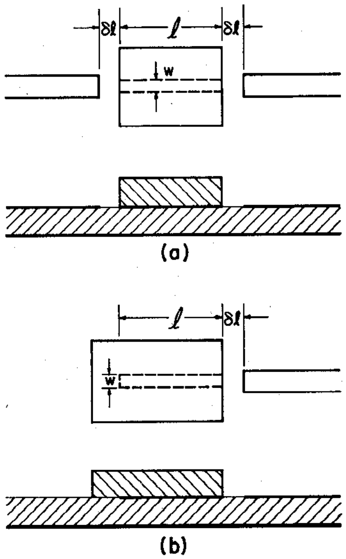

Fig. 2. Microstrip cavity. (a) Transmission type. (b) Reflection type.

more convenient form, that is,

$$\frac{\omega_2}{\omega_1} = \left(\frac{C_1}{C_2}\right)^{1/2} \tag{5a}$$

$$\frac{\omega_1}{Q_1} - \frac{\omega_2}{Q_2} = \frac{G_1}{C_1} - \frac{G_2}{C_2}. \tag{5b}$$

Equations (5a) and (5b) suggest that, instead of measuring the attenuation and phase constants directly, the desired quantities can also be obtained by the measurement of the resonant frequencies and the Q factors of the microstrip cavity for the situations 1) and 2).

The procedures to determine the dielectric quantities, ϵ_2 and tan δ_2, of the unknown materials should be summarized as follows.

a) Place the reference material on the microstrip cavity as shown in Fig. 2. Measure the resonant frequency ω_1 and the Q factor Q_1.

b) Repeat the measurement by replacing the reference material with the unknown material. Obtain ω_2 and Q_2.

c) Compute the values of C_1 and G_1 corresponding to the situation 1) (reference material on the cavity) from the known values of ω, d, ϵ_s, tan $\delta_s, t_1, \epsilon_1$, and tan δ_1. For the computation use equations such as (6) and (7) in the Appendix.

d) Obtain the values of C_2 and G_2 from (5a) and (5b) with the values of $\omega_1, \omega_2, Q_1, Q_2, C_1$, and G_1 derived in steps a)–c).

e) Substitute the obtained values of C_2 into (3a) and solve (3a) for ϵ_2.

f) Substitute the values of C_2, G_2, and ϵ_2 into (3b) and solve (3b) for tan δ_2.

III. MEASUREMENT SETUPS

Fig. 2 shows the schematics of the microstrip cavity circuits. Two types of circuits have been considered. The first one, the transmission type [Fig. 2(a)], is coupled with 50-Ω microstrip lines on both ends of the cavity via small capacitive gaps of width δl. The microwave energy is fed from one of the 50-Ω microstrip lines, while the other 50-Ω line is connected to a power meter or microwave detector for measuring transmission properties of the cavity circuit.

The second type [Fig. 2(b)] makes use of the reflection properties of the cavity where only one 50-Ω microstrip line is used for connecting the cavity with the microwave source and the detector. The resonant frequency and the Q factor of the cavity are determined from the readings of the ratio meter which compares the microwave powers incident to and reflected from the cavity.

In either of the cavity circuits, the width δl of the coupling gaps was chosen to be large enough so that the measured value of Q is essentially the unloaded Q of the cavity. In determining δl, a network analyzer was employed to monitor the degree of coupling. It was found that the coupling coefficient of the typical cavity to the 50-Ω microstrip line was about 0.05. All the circuit components have been constructed on the Rexolite 2200 dielectric plate using copper materials. The cavities are made of a narrow microstrip of width w and length l.

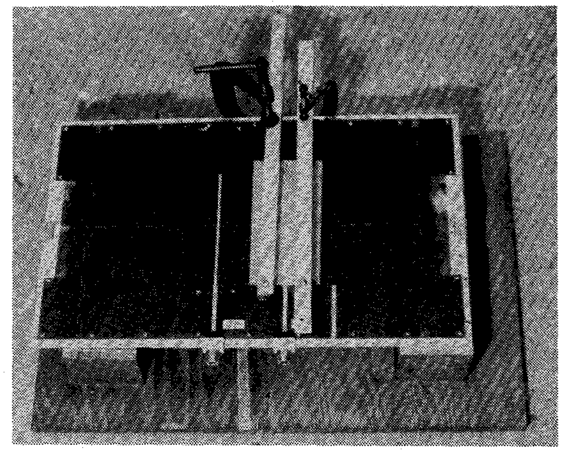

Fig. 3. Actual view of reflection-type cavity used for experiments.

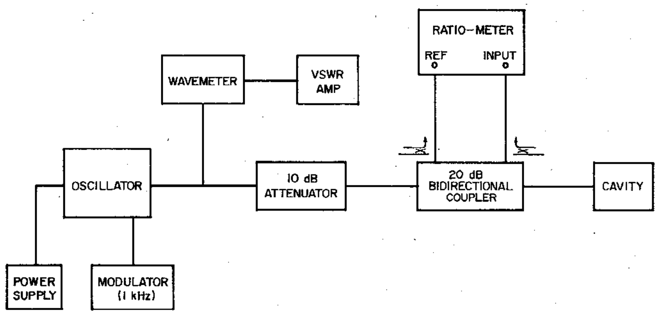

Fig. 4. Schematic diagram of the reflection-type measurements.

It should be noted that the dielectric plates to be measured must be several times wider than the strip width w of the cavity to avoid the end effect of the loading dielectric plate. The length of the plates must be the same as the cavity length l for the transmission-type cavity circuits [Fig. 2(a)]. On the other hand, the length of the plates may be larger than l for the reflection-type cavity [Fig. 2(b)]. There is no restriction on the thickness of the dielectric plates.

Note that the method using the reflection-type cavity is nondestructive in nature, because any dielectric plate can be measured without modifying its original shape as long as it is larger than the minimum size specified above. This nondestructive property is one of the advantages of the present measurement method.

Fig. 3 is the picture of a reflection-type cavity used for the actual measurement. Three 50-Ω microstrip lines are seen, two of which are coupled with the microstrip cavities. A dielectric plate is placed on top of one of the cavities. A considerable amount of pressure should be applied to the plate for the purpose of minimizing the air gap between the plate and the substrate [4]. The air gap is present because the microstrip placed on the substrate has a finite thickness. The effect of thickness was, however, neglected in the analysis.

For crystalline and ceramic materials the elimination of the air gap cannot be attained by the plastic deformation of the material. Hence, unless the extremely thin strip is employed, the present method cannot be readily used for such materials. However, this method could be used if the computer program is designed to include the effect of air gaps.

Fig. 4 shows a schematic diagram of the measuring setups using the reflection-type cavity.

IV. SOME EXAMPLE MEASUREMENTS

The reference material placed on the cavity for obtaining C_1 and G_1 was the same as the substrate, Rexolite 2200; hence, $\epsilon_1 = \epsilon_s$ and tan δ_1 = tan δ_s. The tabulated value of dielectric constant ϵ_s is 2.62 from 0.1 to 10 GHz and the dissipation factor tan δ_s is somewhere between 0.0010 and 0.0014 in the frequency range of 0.2–10 GHz.

TABLE I
TEST RESULTS FOR TRANSMISSION-TYPE CAVITY (300–500 MHz)

Cavity Structure[a]		Polystyrene[b] (7.64 mm thick)		Plexiglass[c] (5.92 mm thick)	
w(mm),	ℓ(mm)	ϵ_2	tan δ_2	ϵ_2	tan δ_2
1.77	210	2.55	0.0009	2.64	0.0073
2.92	210	2.54	0.0010	2.63	0.0059
1.77	185	2.55	0.0011	2.60	0.0042
2.92	185	2.56	0.0011	2.63	0.0068
1.77	160	2.58	0.0012	2.64	0.0067
2.92	160	2.56	0.0007	2.61	0.0066

[a] Substrate is the Rexolite 2200 with 1.59-mm thickness.
[b] Values supplied by the manufacturer: $\epsilon = 2.55$; $\tan \delta = 0.0002$.
[c] Values supplied by the manufacturer: $\epsilon = 2.68$; $\tan \delta = 0.0057$.

TABLE II
RESULTS OF ϵ_2 AND RELATIVE ERROR FOR REFLECTION-TYPE CAVITY (500–1000 MHz)

Cavity Structure			Polystyrene (6.524 mm)		Plexiglass (5.994 mm)	
w(mm),	ℓ(mm),	d(mm)	ϵ_2	relative error(%)	ϵ_2	relative error(%)
3	150	1.524	2.562	+0.49	2.683	+0.11
3	150	1.435	2.532	−0.71	2.601	−2.95
3	120	1.524	2.563	+0.51	2.727	+1.75
3	110	1.524	2.563	+0.51	2.690	+0.37

TABLE III
TEST RESULTS FOR 3- × 120- × 1.524-MM CAVITY

Load	f(MHz)	Q	ε	tan δ
Rexolite	786.1	211.2	2.635	0.0013[a]
Polystyrene	769.0	193.8	2.563	0.0018
Plexiglass	763.0	144.8	2.727	0.0078

[a] Given value.

However, instead of relying on the tabulated value of ϵ_s, the actual ϵ_s value has been experimentally determined. To this end, the resonant frequencies have been measured for the microstrip cavity by loading it first with a Rexolite plate of thickness t and then with two stacked plates of identical thickness t. Equation (5a) was then solved for ϵ_s using (6) with $\epsilon_1 = \epsilon_s$ and $t_1 = t$ or $2t$, respectively. It is another convenient feature of the present method that the value of ϵ_s can be experimentally determined. In the measurement of unknown materials, the experimentally determined ϵ_s value was employed, although the tabulated value of $\tan \delta_s$ has been used.

The measurement using the transmission-type cavity has been performed in the frequency range of 300–500 MHz. The experimentally determined value of ϵ_s was 2.61 and the $\tan \delta_s$ value used in our calculations was 0.0013.

Table I summarizes the measured values of two different materials, i.e., polystyrene and Plexiglas. The consistency of the procedure has been verified by employing several different cavities, and the reliability of the method has been confirmed experimentally. Some inconcistency is noted between the measured values of tan δ and those supplied by the manufacturers. Possibly, the inconsistency can be attributed, among other things, to the fact that the measured Q values are not accurate enough.

The other and possibly major contributing factors for the inconsistency and inaccuracy of tan δ may be as follows.

1) Although the qusi-TEM mode is assumed in the cavity, the discontinuous junctions in the microstrip circuit can excite higher order modes. In addition, at the open ends of the cavity the radiation effect and the surface wave launching may be present. These phenomena are not considered in the present short paper [see (4)] and hence, can be important sources of error in the determination of tan δ.

2) The conductor loss R is a function of frequency. In this short paper, the difference of R was neglected in the cavities loaded with reference and unknown materials. However, since the resonant frequencies of these two situations are ω_1 and ω_2, R does change. Furthermore, the copper loss is normally dominant over the dielectric loss. Therefore, the derivation of (2b) must be more carefully examined. However, the first-order estimate shows the quantity $R_1/L_1 - R_2/L_2$ contributes less than 5-percent error in tan δ values.

The results for ϵ_2 values for the reflection-type cavity are summarized in Table II in which the relative errors are also noted in reference to the values supplied by the manufacturers.

In the reflection-type measurement, an experimentally determined value of ϵ_s was found to be 2.635. The discrepancy of the ϵ_s values for transmission- and reflection-type cavities could be partly due to the effect of air gaps between the substrate and the loading material and partly due to the fact that the two cavities have been prepared from different Rexolite plates.

The determined values of ϵ_2 and $\tan \delta_2$ for several dielectric materials are shown in Table III where measured values of the resonant frequency and the Q values are also given. The factors that affected the results for the transmission-type cavity could also apply to the reflection-type cavity.

Experiments have also been performed for several other materials and it was found that the measured data agree reasonably well with the data supplied by the manufacturers.

The typical computation time for deriving both ε and tan δ from the measured values of resonant frequencies and Q's was about 120 s on a CDC G-20 computer, which is about 10 times slower than the IBM 360/75.

V. CONCLUSIONS

An efficient nondestructive method for measuring the dielectric properties has been explained. The accuracy of the dielectric constant so obtained is usually better than 3 percent (often as good as 0.5 percent), while that of the dissipation factor is only moderate. Several possibilities for improving the latter are: 1) improve the accuracy of the Q measurement; 2) employ substrates of higher dielectric constant to reduce possible radiation losses; and 3) investigate the effect of air gaps.

APPENDIX

CALCULATION OF THE LINE CAPACITANCE AND THE LINE CONDUCTANCE

A substantial amount of information is available on the calculation of the line capacitance of microstrip lines [11]–[14]. In this short paper, the method developed by Yamashita and Mittra [13] and Yamashita [14] is applied. Consider the cross section of the microstrip line shown in Fig. 1. The strip is assumed to be infinitely thin. All the conductors are assumed lossless. Furthermore, for the purpose of capacitance calculation, the filling media are assumed to be lossless.

The variational expression for the line capacitance C_i is

$$\frac{1}{C_i} = \frac{1}{2\pi\epsilon_0 q^2} \int_{-\infty}^{\infty} \tilde{g}_i(\beta)\tilde{\rho}^2(\beta)\, d\beta \tag{6}$$

where q is the total charge on the strip

$$\frac{\tilde{\rho}(\beta)}{q} = \frac{8}{5}\left[\frac{\sin(\beta w/2)}{\beta w/2}\right] + \frac{12}{5(\beta w/2)^2}\left[\cos(\beta w/2) - \frac{2\sin(\beta w/2)}{\beta w/2} + \frac{\sin^2(\beta w/4)}{(\beta w/4)^2}\right]$$

$$\tilde{g}_i(\beta) = \frac{1 + \epsilon_i \coth(\beta t_i)}{\beta\{\epsilon_i[\epsilon_i + \coth(\beta t_i)] + \epsilon_s \coth(\beta d)[1 + \epsilon_i \coth(\beta t_i)]\}}$$

and $i = 1$ or 2, corresponding to Fig. 1(a) or (b), respectively.

When a perturbation technique is used for the microstrip line filled with the materials that have small losses ($\sigma \ll \omega\epsilon$), the following expression for the line conductance G_i can be derived from (6):

$$\frac{G_i}{C_i^2} = \frac{1}{2\pi\epsilon_0 q^2}\int_{-\infty}^{\infty} \frac{\{\sigma_i[2\epsilon_i + (1+\epsilon_i^2)\coth(\beta t_i)] + \sigma_s \coth(\beta d)[1 + \coth(\beta t_i)]^2\}}{\beta\{\epsilon_i[\epsilon_i + \coth(\beta t_i)] + \epsilon_s \coth(\beta d)[1 + \epsilon_i \coth(\beta t_i)]\}^2}\cdot\tilde{\rho}^2(\beta)\, d\beta, \qquad i = 1 \text{ or } 2 \qquad (7)$$

where σ_s and σ_i are the conductivities of the substrate and the loading material, respectively.

ACKNOWLEDGMENT

The author wished to thank Prof. J. D. Dyson and Prof. R. Mittra for fruitful discussions, and M. Sato and J. J. Sweeney for experimental assistance.

REFERENCES

[1] J. S. Yu, L. Peter, Jr., and D. A. Castello, "A refractive index chart for a scattering sphere," *IEEE Trans. Antennas Propagat.*, vol. AP-18, pp. 75–83, Jan. 1970.
[2] D. J. Burr, "Measurement of the complex dielectric constant from resonance in the radar cross section of a dielectric sphere," M.S. thesis, Dep. Elec. Eng., Univ. Ill., Urbana, 1971.
[3] H. E. Stinehelfer, Sr., "Ridge waveguide resonant cavity for measuring dielectric constants," *Patent Gazette*, 3,384,814, May 21, 1968.
[4] M. Olyphant, Jr., and J. H. Ball, "Strip-line method for dielectric measurements at microwave frequency," *IEEE Trans. Elec. Insul.*, vol. EI-5, pp. 26–32, Mar. 1970.
[5] L. S. Napoli and J. J. Hughes, "A simple technique for the accurate determination of the microwave dielectric constant for microwave integrated circuit substrates," *IEEE Trans. Microwave Theory Tech.* (Corresp.), vol. MTT-19, pp. 664–665, July 1971.
[6] J. Q. Howell, "A quick accurate method to measure the dielectric constant of microwave integrated-circuit substrates," *IEEE Trans. Microwave Theory Tech.* (Short Paper), vol. MTT-21, pp. 142–143, Mar. 1973.
[7] P. H. Ladbrooke, M. H. N. Potok, and E. H. England, "Coupling errors in cavity-resonance measurements on MIC dielectrics," *IEEE Trans. Microwave Theory Tech.* (Short Paper), vol. MTT-21, pp. 560–562, Aug. 1973.
[8] R. Mittra and T. Itoh, "A new technique for the analysis of the dispersion characteristics of microstrip lines," *IEEE Trans. Microwave Theory Tech.*, vol. MTT-19, pp. 47–56, Jan. 1971.
[9] S. Ramo and J. R. Whinnery, *Fields and Waves in Modern Radio*. New York: Wiley, 1953.
[10] T. Itoh, R. Mittra, and R. D. Ward, "A method for computing edge capacitance of finite and semifinite microstrip lines," *IEEE Trans. Microwave Theory Tech.* (Short Paper), vol. MTT-20, pp. 847–849, Dec. 1972.
[11] H. A. Wheeler, "Transmission-line properties of parallel strips separated by a dielectric sheet," *IEEE Trans. Microwave Theory Tech.*, vol. MTT-13, pp. 172–185, Mar. 1965.
[12] H. E. Stinehelfer, Sr., "An accurate calculation of uniform microstrip transmission lines," *IEEE Trans. Microwave Theory Tech.* (*Special Issue on Microwave Integrated Circuits*), vol. MTT-16, pp. 439–444, July 1968.
[13] E. Yamashita and R. Mittra, "Variational method for the analysis of microstrip lines," *IEEE Trans. Microwave Theory Tech.*, vol. MTT-16, pp. 251–256, Apr. 1968.
[14] E. Yamashita, "Variational method for the analysis of microstrip-like transmission lines," *IEEE Trans. Microwave Theory Tech.*, vol. MTT-16, pp. 529–535, Aug. 1968.

Circular Bends in Dielectric Frame Beam Waveguides

P. F. CHECCACCI, R. FALCIAI, AND A. M. SCHEGGI

***Abstract*—An investigation is described on circular bends in beam waveguides constituted by dielectric frames [5]. A uniform bending of the guide axis is obtained by tilting each frame by a small angle; however, due to the phase correction performed by the dielectric frame, the losses introduced by the bending can be made lower than those of an analogously bent iris waveguide. A numerical analysis is performed on the basis of the analogy between beam waveguides and open resonators which permits the assessment, in a number of cases, of the maximum permissible amount of tilting and the corresponding optimum frame dimensions in view of acceptable losses. The losses due to mode conversion are also evaluated when considering the connection between a straight and a curved section of the waveguide.**

Manuscript received September 12, 1973; revised January 3, 1974.
The authors are with Consiglio Nazionale Delle Ricerche, Istituto di Ricerca sulle Onde Eletromagnetiche, Florence, Italy.

It is well known that beam waveguides cannot be made to follow a curved path like tubular waveguides, but bends can be obtained by the use of prisms or mirrors. However, curvatures with large radii (like those encountered to follow the ground contour or to avoid obstacles along the path) can be achieved by lateral displacements of the elements in a lens waveguide or by a sequence of small angle changes at each aperture of an iris waveguide [1]–[4].

The present short paper is concerned with an investigation of circular bends in dielectric frame beam waveguides [5], [6], along with some considerations on the transition between straight and curved sections of the guide.

The investigation has been carried out on the basis of the analogy between open resonators and beam waveguides. In this respect it is expedient to recall that the dielectric frame beam waveguide is equivalent to the step rimmed Fabry–Perot resonator [6], [7]. The rims control the field at the edges of the mirrors giving rise to a periodical enhancement or decrease of the losses as the rim thickness varies. Such control can also be made at each edge almost independently and without altering appreciably the overall field shape.

A beam waveguide of constant radius of curvature is equivalent to a tilted rimmed mirror resonator. The diffraction losses for the fundamental mode of a Fabry–Perot resonator with tilted mirrors have been evaluated for different amounts of tilting and by varying the Fresnel number. Such losses (Fig. 1) have been compared with those evaluated for the same resonators in the presence of rims. The rim dimensions (width and thickness) here are those corresponding to minimum loss and, in fact, the losses of the rimmed resonator are much lower than those in the absence of rim. This decrease is due to the rims placed at the largest distance edges of the mirrors which limit the field spill-over caused by the tilting. Equal curves are obtained by placing the rims also at the nearest distance edges, their effect being negligible due to the extremely low value of the field at that side. Consequently, this rim can be suppressed; however, when considering the corresponding beam waveguides (Fig. 2), this rim is maintained for constructive reasons and the curved section waveguide results constituted by a number of cells with frames tilted one with respect to the other by the same angle. The guidance in such curved sections is achieved through the combined effects of frame tilting and phase-front correction performed by the frame itself at the external side of the curve.

The diffraction losses per cell are those of the equivalent resonator (Fig. 1). However, other losses are present, and precisely, losses due to mode conversion at the transition between straight and curved sections and vice versa, as well as reflection losses due to impedance mismatching at the same transitions. These last ones will be neglected in our treatment. The mode conversion losses of interest in this case are those relative to the zero mode which at the transitions is partially converted into higher order ones. The energy lost in this conversion was evaluated by considering the ratio between the energy of the zero mode for the input cell and the energy of the resultant zero mode of the output cell.

Fig. 3 shows the mode conversion losses in the case $N = 2.5$ plotted versus ϵ (amount of tilting of the output cell) for different values of ϵ_0 (amount of tilting of the input cell). The value $\epsilon_0 = 0$ corresponds to the particular case of a transition between a straight and a tilted cell. Values of the radii of curvature corresponding to the considered values of ϵ_0 and ϵ are also indicated which are valid in